1 **Intrabacterial regulation of a cytotoxic effector by its cognate metaeffector promotes**

2 ***Legionella pneumophila* virulence**

3

4 Deepika Chauhan,[a]* Ashley M. Joseph,[a] Stephanie R. Shames[a]#

5

6 [a]Division of Biology, Kansas State University, Manhattan, Kansas 66506 USA

7

8 Running title: Intrabacterial effector regulation by a metaeffector

9

10 #Address correspondence to Stephanie R. Shames, sshames@ksu.edu

11

12 *Present address: Department of Diagnostic Medicine and Pathobiology, College of Veterinary

13 Medicine, Kansas State University, Manhattan, Kansas 66506

14

Abstract

Legionella pneumophila is a natural pathogen of unicellular protozoa that can opportunistically infect macrophages and cause Legionnaires' Disease. Intracellular replication is driven by hundreds of bacterial effector proteins that are translocated into infected host cells by a Dot/Icm type IV secretion system. *L. pneumophila* effectors are temporally regulated in part by a unique family of translocated regulatory effectors, termed metaeffectors, which bind and modulate the function of a cognate effector in host cells. We discovered that regulation of the cytotoxic effector SidI by its metaeffector, MesI, is critical for *L. pneumophila* virulence in natural and opportunistic hosts. MesI binds and negatively regulates SidI activity *in vitro* but how dysregulation of SidI impairs *L. pneumophila* intracellular replication is unclear. Using a chromosomally-encoded inducible expression system, we discovered that dysregulation of SidI, via loss of MesI, was toxic to *L. pneumophila.* SidI enzymatic activity was required for toxicity since *L. pneumophila* growth was unaffected by induced expression of a catalytically inactive *sidI* allele. We found MesI translocation into host cells was dispensable for intracellular replication and that MesI-deficient bacteria were rapidly degraded within host cells. Together, our data suggest a unique role for intrabacterial effector regulation by a translocated metaeffector in *L. pneumophila* virulence.

32 **Importance**

33 *Legionella pneumophila* replicates within phagocytic host cells using hundreds of effector protein
34 virulence factors, which canonically subvert the function of host proteins and pathways. *L. pneu-*
35 *mophila* encodes a unique family of translocated effectors called metaeffectors, which bind and
36 regulate the function of a cognate effector in host cells. The metaeffector MesI promotes *L. pneu-*
37 *mophila* virulence by regulating the cytotoxic effector SidI; however, the MesI regulatory mecha-
38 nism is poorly understood. We discovered a unique intrabacterial role for MesI in *L. pneumophila*
39 virulence. When uncoupled from MesI, SidI was toxic to *L. pneumophila in vitro* and triggered
40 robust bacterial degradation in host cells. Importantly, translocation of MesI was dispensable for
41 intracellular replication, demonstrating that intrabacterial regulation of SidI contributes to *L.*
42 *pneumophila* virulence. These data show a unique and important role for MesI regulation of SidI
43 within the bacterium, which challenges the dogma that effectors function exclusively within host
44 cells.

45

46

47 **Introduction**

48 *Legionella pneumophila* is ubiquitous in freshwater environments where it parasitizes and repli-
49 cates within free-living protozoa. Co-evolution with environmental phagotrophs have conferred
50 on *L. pneumophila* the ability to replicate within mammalian macrophages, which results in a se-
51 vere inflammatory pneumonia called Legionnaires' Disease (1–3). Within host cells, *L. pneumoph-*
52 *ila* replicates within an endoplasmic reticulum (ER)-derived compartment called the *Legionella-*
53 containing vacuole (LCV), which avoids endocytic maturation and fusion with lysosomes (4, 5).
54 Biogenesis of the LCV is facilitated through the activity of over 300 effector proteins, bacterial
55 virulence factors translocated into host cells through a Dot/Icm type IV secretion system (T4SS)
56 (6). Dot/Icm-translocated effectors are critical for *L. pneumophila* virulence in natural and oppor-
57 tunistic hosts (7); however, the role of most effectors remains poorly understood due primarily to
58 functional redundancy and rarity of virulence phenotypes in laboratory infection models.

59 Many Gram-negative bacterial pathogens employ effector proteins as part of their virulence
60 strategy. Canonically, effector proteins function by targeting host proteins and subverting cellular
61 pathways to the benefit of the pathogen; however, *L. pneumophila* encodes a unique family of
62 translocated effectors termed metaeffectors, which bind and regulate other *L. pneumophila* effec-
63 tors within host cells (8, 9). Metaeffectors are a key component of *L. pneumophila* pathogenicity
64 since several are required for intracellular replication but how most metaeffectors promote viru-
65 lence is poorly understood.

66 We discovered that regulation of the effector SidI (Lpg2504) by its cognate metaeffector,
67 MesI (Lpg2505), is critical for *L. pneumophila* virulence (10). Like most *L. pneumophila* effectors,
68 loss of SidI has no effect on virulence in laboratory infection models; however, loss-of-function

69 mutation in *mesI* (Δ*mesI*) uniquely attenuates *L. pneumophila* virulence in amoebae, macrophages,
70 and mouse models of Legionnaires' Disease only when SidI is produced (10). SidI is a cytotoxic
71 glycosyl hydrolase that inhibits eukaryotic mRNA translation (11, 12). MesI binds SidI with high
72 affinity, suppresses its toxicity, and blocks SidI-mediated translation inhibition *in vitro* (12). The
73 requirement for MesI is relieved when *sidI* is deleted (Δ*sidI*); however, a single amino acid substi-
74 tution that renders SidI non-toxic and catalytically inactive (R453P) is also sufficient to restore
75 replication of MesI-deficient *L. pneumophila* (10). These data have provided key biochemical in-
76 sights into the MesI regulatory mechanism but how MesI regulation of SidI promotes intracellular
77 replication is still unclear.

78 In this study, we made the surprising discovery that MesI promotes *L. pneumophila* viru-
79 lence by regulating SidI intrabacterially. SidI was toxic to *L. pneumophila* when uncoupled from
80 MesI *in vitro*. We found that MesI translocation was dispensable for *L. pneumophila* intracellular
81 replication and MesI-deficient bacteria are rapidly degraded in host cells. These data suggest a
82 unique and important role for interkingdom effector regulation in *L. pneumophila* virulence.
83

84

85 **Results**

86 **Overexpression of *sidI* impairs *L. pneumophila* growth *in vitro*.** We discovered that the *L. pneu-*
87 *mophila* metaeffector MesI promotes bacterial intracellular replication by regulating its cognate
88 effector SidI (10), but how SidI dysregulation attenuates *L. pneumophila* virulence is unclear. A *L.*
89 *pneumophila* Δ*mesI* mutant is impaired for intracellular replication but virulence is restored by *sidI*
90 chromosomal deletion (Δ*sidI*Δ*mesI*) or catalytic inactivation (*sidI*$_{R453P}$Δ*mesI*). We initially validated
91 that dysregulation of SidI impairs *L. pneumophila* intracellular replication by plasmid-based ge-
92 netic complementation of the Δ*sidI* mutation. We infected primary bone marrow-derived macro-
93 phages (BMDMs) from *Nlrc4*$^{-/-}$ mice, which are permissive to flagellated *L. pneumophila* (13, 14).
94 Indeed, induced expression of *sidI* from a complementing plasmid severely attenuated *L. pneu-*
95 *mophila* replication within BMDMs (**Fig 1A**). Interestingly, we had to induce *sidI* expression at the
96 time of infection since we were unable to culture *L. pneumophila* Δ*sidI*Δ*mesI* (p*sidI*) on inducing
97 media. Inducible plasmid-based genetic complementation is an established technique to fulfill
98 molecular Koch's postulates and we routinely culture *L. pneumophila* on inducing media (10, 12,
99 15–17). We hypothesized that overexpression of SidI adversely affects bacterial physiology. In-
100 deed, *L. pneumophila* harboring p*sidI* was unable to replicate in broth under inducing conditions
101 but not in the absence of induction (**Fig 1B**). Impaired growth resulted from SidI enzymatic ac-
102 tivity since induced the catalytically inactive *sidI*$_{R453P}$ allele did not affect *L. pneumophila* growth
103 (**Fig 1B**). Our initial interpretation was that dysregulation of SidI does not adversely affect *L.*
104 *pneumophila* physiology since *L. pneumophila* Δ*mesI* is not attenuated for growth *in vitro* (10). How-
105 ever, *sidI* expression in broth grown bacteria is ~ 3-fold lower than expression during intracellular

106 replication (18), which may be insufficient to impair *L. pneumophila* growth. Induced expression
107 of an effector gene has not previously been associated with impaired bacterial growth and these
108 data suggest that SidI enzymatic activity is deleterious to *L. pneumophila* when stoichiometrically
109 uncoupled from MesI.
110
111 **MesI rescues the SidI-mediated growth defect *in vitro*.** MesI suppresses SidI toxicity in yeast
112 (10); thus, we hypothesized that MesI also suppresses SidI toxicity in *L. pneumophila*. To test this
113 hypothesis, we generated *L. pneumophila* strains that enable tightly controlled inducible expres-
114 sion of the *sidI-mesI* locus from its endogenous position in the chromosome. We inserted the *araC-*
115 *araBAD* (araBAD) promoter and an in-frame *3xflag* epitope tag directly upstream of *sidI* in the
116 chromosome of WT, Δ*mesI*, and *sidI*$_{R453P}$Δ*mesI L. pneumophila* strains (**Fig 2A**). Kinetics and abun-
117 dance of 3xFLAG-SidI fusion protein production was consistent between strains and only ob-
118 served under arabinose-inducing conditions (**Fig 2B**). We observed a tightly controlled increase
119 in araBAD-mediated *sidI* expression relative to endogenous levels (**Fig 2C**). The ~4-fold increase
120 in *sidI* expression from the araBAD promoter is more physiologically relevant than the >10-fold
121 increase in expression from the P*tac* promoter (**Fig 2C**) (18). Thus, we have established *L. pneu-*
122 *mophila* strains in which we can control expression of *sidI* and *mesI* in their native stoichiometry
123 and endogenous locus in the chromosome.
124 We leveraged our *L. pneumophila* araBAD strains (**Fig 2A**) to test the hypothesis that stoi-
125 chiometric production of MesI abrogates SidI-mediated growth attenuation. We quantified rep-
126 lication our *L. pneumophila* araBAD strains under inducing and non-inducing conditions and
127 found that induced expression of *sidI,* but not the inactive *sidI*$_{R453P}$ allele, significantly attenuated

128 bacterial growth only when uncoupled from *mesI* in broth culture (**Fig 3A**) and within BMDMs
129 (**Fig 3B**). Thus, the SidI-mediated growth defect is suppressed by MesI.
130
131 **MesI suppresses SidI intrabacterial toxicity.** SidI impairs *L. pneumophila* growth, but it is unclear
132 whether SidI is bacteriostatic or bactericidal. SidI is toxic to yeast (11); thus, we tested the hypoth-
133 esis that SidI is bactericidal when uncoupled from MesI. *L. pneumophila* araBAD strains (**Fig 2A**)
134 were grown for 24 h under arabinose inducing or non-inducing conditions in broth and viability
135 was evaluated using LIVE/DEAD viability staining and confocal microscopy (**Fig 4**). Very few
136 dead bacteria were observed under non-inducing conditions or when induced *sidI* expression
137 was coupled with *mesI* (araBAD-WT) (**Fig 4**). However, significantly more dead bacteria were
138 observed when enzymatically active *sidI* was uncoupled from *mesI* under inducing conditions
139 (**Fig 4**). These data suggest that SidI toxicity is conserved across the kingdoms of life and sup-
140 pressed by MesI.
141
142 **Intrabacterial regulation of SidI by MesI is sufficient for *L. pneumophila* virulence.** Based on
143 our observation that SidI is toxic to *L. pneumophila* when uncoupled from MesI, we hypothesized
144 that MesI intrabacterial regulation of SidI is sufficient for *L. pneumophila* virulence. We tested this
145 by evaluating whether an intrabacterially-retained MesI mutant could complement the Δ*mesI* mu-
146 tation. We generated an allele of *mesI* lacking 10 amino acids from its extreme carboxy terminus;
147 these amino acids are dispensable for SidI binding and contains the putative E-block Dot/Icm
148 translocation signal (19, 20). We cloned this allele into a complementing plasmid downstream of
149 a *3xflag* epitope tag (p*mesI*$_{\Delta 10}$). We evaluated 3xFLAG-MesIΔ10 translocation using Western blot

150 to visualize its abundance in saponin-soluble or -insoluble lysate fractions from *L. pneumophila*-
151 infected cells, a technique routinely used to evaluate effector secretion, since saponin solubilizes
152 eukaryotic membranes but minimally lyses *L. pneumophila* (21, 22). HEK293 FcγRII cells were in-
153 fected with antibody-opsonized *L. pneumophila* harboring either p*mesI* or p*mesI*$_{\Delta 10}$. 3xFLAG-
154 MesIΔ10 was not translocated since it was retained in the insoluble fraction (pellet) and not pre-
155 sent in saponin-soluble lysate fractions (**Fig 5A**). As expected, wild-type MesI was secreted into
156 host cells since it was present within saponin-soluble lysate fractions (**Fig 5A**). Isocitrate dehy-
157 drogenase (ICDH) and β-actin were used as bacterial lysis and loading controls, respectively. We
158 also confirmed that MesIΔ10 interacts with SidI since it was retained by SidI on beads similarly
159 to full-length MesI (**Fig S1**).

160 To evaluate a role for intrabacterial SidI regulation by MesI in *L. pneumophila* virulence,
161 we tested whether the *mesI*$_{\Delta 10}$ allele genetically complements that Δ*mesI* mutation. We infected
162 BMDMs and quantified replication of wild-type *L. pneumophila* and Δ*mesI* strains harboring p*mesI*,
163 p*mesI*$_{\Delta 10}$, or empty plasmid vector (pEV). We were able to genetically complement the Δ*mesI* with
164 the *mesI*$_{\Delta 10}$ allele, demonstrating that MesI translocation into host cells is not necessary for *L. pneu-*
165 *mophila* intracellular replication (**Fig 5B**). These data suggest that intrabacterial regulation of SidI
166 by MesI is sufficient for *L. pneumophila* virulence.

167

168 **MesI-deficient bacteria are degraded within host cells.** We found that MesI suppresses intrabac-
169 terial SidI toxicity and that MesI translocation into host cells is dispensable for *L. pneumophila*
170 intracellular replication. Since SidI is also toxic to eukaryotic cells, we initially postulated that the
171 virulence defect associated with loss of MesI results from SidI toxicity in host cells. However, we

172 were unable to detect SidI-mediated cytotoxicity in *L. pneumophila*-infected BMDMs (**Fig S2**) and
173 our new data suggest a potential role for MesI suppression of intrabacterial SidI toxicity in *L.*
174 *pneumophila*'s virulence strategy.

175 Dead and dying bacterial are rapidly degraded within host lysosomes; thus, we rational-
176 ized that MesI-deficient bacteria would be robustly degraded within host cells. Degraded *L. pneu-*
177 *mophila* are easily identified using immunofluorescence microscopy since they have lost their rod
178 shape and appear instead as diffuse puncta when cells are stained with a *Legionella*-specific anti-
179 body (23, 24). Thus, we used immunofluorescence microscopy and blinded scoring to quantify
180 degradation of *L. pneumophila* Δ*mesI* within BMDMs. We infected BMDMs and compared kinetics
181 of *L. pneumophila* Δ*mesI* degradation to virulent *L. pneumophila* and *L. pneumophila* Δ*dotA*, which is
182 unable to evade lysosomal degradation (25). After 1 h of infection, most bacteria retained their
183 rod shape and there were no differences between *L. pneumophila* strains; however, at 8 h post-
184 infection, significantly more *L. pneumophila* Δ*mesI* were degraded compared to both wild-type and
185 Δ*dotA* control strains (**Fig 6**). It is unlikely that bacterial degradation was accompanied by host
186 cell death since macrophages harboring degraded bacteria had normal nuclear morphology (**Fig**
187 **6**). The robust degradation of *L. pneumophila* Δ*mesI* compared to the avirulent Δ*dotA* strain sug-
188 gests a mechanism of bacterial attenuation distinct from the inability to subvert endocytic matu-
189 ration.

190

191 **Discussion**

192 This study supports a unique model whereby the *L. pneumophila* metaeffector MesI drives viru-
193 lence by intrabacterial regulation its cognate effector SidI (**Fig 7**). Several *L. pneumophila* effectors

194 are toxic to eukaryotic cells; however, effector bactericidal activity in *L. pneumophila* has not been
195 previously observed. Furthermore, our data challenge the dogma that metaeffectors promote *L.*
196 *pneumophila* virulence by functioning exclusively within host cells. SidI and MesI bear resem-
197 blance to canonical toxin-antitoxin (TA) and effector-immunity (E-I) pairs (26–28); however, they
198 are distinct since anti-toxin/immunity proteins, by definition, are not secreted(29). This also dis-
199 tinguishes MesI from canonical chaperones, which remain intrabacterial (30). MesI negatively
200 regulates SidI subversion of eukaryotic homeostasis (12) and a role for host cell pathways in the
201 MesI regulatory mechanism cannot be fully excluded (**Fig 7**). However, our data suggest a novel
202 mechanism by which *L. pneumophila* virulence hinges on effector regulation by a metaeffector
203 within the bacterium.
204
205 Interkingdom SidI toxicity suggests that its target is highly conserved between *L. pneumophila* and
206 host cells. SidI is one of at least seven *L. pneumophila* effectors that subvert host protein synthesis
207 (11, 31), one of the most conserved cellular processes across the kingdoms of life (32). Effector-
208 mediated suppression of host mRNA translation is important for *L. pneumophila*'s acquisition of
209 host-derived amino acids, which are essential for intracellular replication and the main driver of
210 bacterial phase switching within host cells (23, 33). The mechanism by which SidI inhibits protein
211 synthesis is unclear; however, SidI binds eEF1A and likely functions as a mannosyltransferase,
212 so it is tempting to speculate that SidI blocks translation by modifying eEF1A (11, 12). However,
213 the functional significance of eEF1A binding remains unclear since it is unaffected by MesI and
214 insufficient for translation inhibition (11, 12). *L. pneumophila* has evolved strategies to prevent
215 intrabacterial suppression of translation. For example, the effector Lgt1 blocks eukaryotic

216 translation by glycosylating eukaryotic elongation factor (eEF)1A on Ser53, which is conserved
217 in eukaryotes but not the bacterial eEF1A homolog, EF-Tu (34, 35). The mechanistic underpin-
218 nings of intrabacterial MesI activity is unclear; however, it is tempting to speculate that MesI may
219 function in part to preserve protein synthesis within the bacterium.
220
221 Recent work has challenged the dogma that bacterial effectors function exclusively within host
222 cells. Hardwidge and colleagues revealed that the pathogenic *E. coli* effector NleB and *Salmonella*
223 *enterica* Typhimurium effector SseK1 function intrabacterially. NleB confers resistance to oxida-
224 tive stress and SseK1 confers resistance to methylglyoxal and regulates UDP-GlcNAc biosynthe-
225 sis (36–38). The pathogenic E. coli effector NleC can also function intrabacterially, but the endog-
226 enous, biologically relevant substrates are unknown (39). Our data suggest that intrabacterial
227 MesI activity confers a fitness advantage on *L. pneumophila* by suppressing intrabacterial SidI ac-
228 tivity. However, MesI is produced at later time points than SidI when *L. pneumophila* is grown in
229 broth (19), suggesting that low levels of SidI activity within the bacterium may be beneficial at
230 early stages of the *L. pneumophila* lifecycle. Indeed, there is emerging evidence that bacterial TA
231 pairs can shape pathogen physiology by modulating post-transcriptional gene expression (40).
232 However, this activity must be highly regulated by the antitoxin to prevent toxicity. Thus, it is
233 tempting to speculate that SidI and MesI are an ancient TA pair that have been co-opted by the
234 T4SS to subvert both host and pathogen physiology.
235
236 Our data challenge our initial assumption that MesI promotes *L. pneumophila* intracellular repli-
237 cation by preventing SidI-mediated host cell toxicity. We found no SidI-mediated differences in

238 host cell death and observed that macrophages MesI-deficient bacteria had normal morphology.
239 Interestingly, McCloskey *et al* recently proposed a model whereby MesI negatively regulates SidI
240 translocation into host cells (19). MesI binds the extreme C-terminus of SidI, which encodes the
241 canonical E-block Dot/Icm translocation signal (12, 19, 41). McCloskey *et al.* recently suggested
242 that MesI negatively regulates SidI secretion from *L. pneumophila*. However, SidI secretion was
243 not further attenuated when the relative abundance of MesI was increased (19). Furthermore, we
244 did not detect any MesI-mediated differences in SidI translocation from *L. pneumophila* using an
245 the established adenylate cyclase (CyaA) reporter (12). This discrepancy may be a consequence
246 of differences in experimental conditions. Further investigation is required to define the impact
247 of MesI on SidI translocation and the potential role of this activity in the MesI regulatory mecha-
248 nism and *L. pneumophila* virulence.
249
250 Together, this study revealed a unique role for intrabacterial regulation of a translocated effector
251 by its cognate metaeffector in *L. pneumophila* virulence. Our data, in the context of previously
252 published studies (11, 12), suggest that SidI's target is conserved between host and pathogen.
253 Recent phylogenetic analysis suggests ancient and extensive co-evolution between the order *Le-*
254 *gionellales,* which includes *Legionella* spp., and unicellular eukaryotes (42). Thus, metaeffectors
255 may represent an ancient mechanism evolved by pathogenic bacteria for adaptation to eukaryotic
256 hosts.
257
258 **Materials & Methods**

259 **Bacterial strains, plasmids, primers, and culture conditions.** *Escherichia coli* Top10 (cloning),
260 DH5αλ*pir* (allelic exchange) and BL21 (DE3) (protein production) were maintained at 37˚C in
261 Luria-Bertani (LB) medium supplemented with appropriate antibiotics for plasmid maintenance
262 [50 μg mL^{-1} kanamycin, 25 μg mL^{-1} chloramphenicol, or 100 μg mL^{-1} ampicillin]. Protein produc-
263 tion in *E. coli* BL21 (DE3) was induced with 1 mM isopropyl-β-D-1-thiogalactopyranoside (IPTG).
264 All *Legionella pneumophila* strains in this study were derived from *L. pneumophila* Philadel-
265 phia-1 SRS43 (10) and cultured at 37˚C on charcoal–N (2-acetamido)-2-aminoethanesulfonic acid
266 (ACES)-buffered yeast extract (CYE) supplemented with L-cysteine and ferric pyrophosphate as
267 described previously (43). Single colonies were isolated after 4 days of growth on CYE agar and
268 used to generate 48 h heavy patches of bacteria. Where indicated, liquid cultures were grown
269 from heavy-patched bacteria at 37°C in L-cysteine- and ferric pyrophosphate-supplemented
270 ACES buffered yeast extract broth (AYE) (44). Media were supplemented with 10 μg mL-1 chlo-
271 ramphenicol (plasmid maintenance), 10 μg mL-1 kanamycin (allelic exchange), 1 mM IPTG (P*tac*
272 gene expression), or 0.6-2% L-arabinose (w/v; paraBAD gene expression).
273 Plasmids and oligonucleotide primers used in this study are listed in **Table 1** and **Table**
274 **2**, respectively.
275
276 **Molecular cloning and strain construction.** *L. pneumophila* gDNA was isolated using the Illustra
277 genomicPREP DNA spin kit (GE Healthcare) and used as a template for cloning *sidI* and *mesI* into
278 the indicated plasmid vectors. *sidI* was amplified from *L. pneumophila* gDNA using SidIBamHI-
279 F/SidISphI-R, which includes 60 base-pairs (bp) downstream of the *sidI* open reading frame, and
280 cloned as a BamHI/SphI fragment into pJB1806 (45) or downstream of an in-frame *3xflag* epitope

281 tag in pSN85 (46) to generate pJB1806::*sidI* (p*sidI*) and pSN85::*sidI*. To generate p*sidI*$_{R453P}$, p*sidI* was
282 mutagenized using site-directed mutagenesis with primer pairs SidIR453P-sense/SidIR453P-
283 asense (10). To generate p*mesI* complementation plasmids, *mesI* and *mesI*$_{\Delta 10}$ open reading frames
284 were amplified from *L. pneumophila* gDNA using MesIBglII-F/MesISphI-R or MesIBglII-
285 F/MesIΔ10SphI-R primer pairs, respectively, and cloned into pSN85 in-frame with the *3xflag*
286 epitope tag. Ligations were transformed into chemically competent *E. coli* Top10 and sequences
287 confirmed by Sanger sequencing (Eton Biosciences). *L. pneumophila* complementation strains were
288 generated by electroporation of plasmids into competent *L. pneumophila* strains using a BioRad
289 Gene Pulser at 2.4 kV, 200 Ω, and 0.25 μF and plated on CYE supplemented with 10 μg mL^{-1}
290 chloramphenicol.

291 For production of recombinant His$_6$-Myc-MesIΔ10, *mesI*Δ10 was amplified from *L. pneu-*
292 *mophila* gDNA using MesIT7SalI-F/MesIΔ10NotI-R and cloned as a SalI/NotI fragment into
293 pT7HMT (47) downstream of an in-frame His$_6$-Myc epitope tag. pT7HMT::*mesI* and pGEX::*sidI*
294 were generated previously (**Table 2**) (12). Ligation reactions were transformed into chemically
295 competent *E. coli* Top10 and sequences were confirmed by Sanger sequencing (Eton Biosciences).

296 The *dotA* open reading was deleted from the *L. pneumophila* chromosome using allelic ex-
297 change, as described (48). To generate a clean in-frame deletion of *dotA*, 5′ and 3′ regions flanking
298 the *dotA* open reading frame (726 bp upstream and 1,012 bp downstream) were amplified using
299 DotAKOSacI-F/DotAKONotI-R and DotAKONotI-F/DotAKOSalI-R to generate SacI/NotI and
300 NotI/SalI fragments which were ligated into SacI/SalI digested pSR47s to generate pSR47s::Δ*dotA*,
301 which was conjugated into *L. pneumophila* SRS43 for selection of double crossover events, as

302 described. Sequences were confirmed by Sanger sequencing (Eton Biosciences) and the ΔdotA
303 phenotype was confirmed by comparison the established SRS43 *dotA*::Tn strain (10).
304 For allelic exchange to insert the paraBAD promoter and a *3xflag* epitope tag upstream of
305 *sidI* in the *L. pneumophila* chromosome, overlapping primers were used to generate a fusion con-
306 struct consisting of 1,000 bp upstream of *sidI* (SidIUTR-F/SidIUTR-R; from *L. pneumophila* gDNA),
307 araBAD promoter [araC-pBAD-F/araC-pBAD-R; from pMRBAD::z-CspGFP (a gift from Dr. Brian
308 McNaughton; Addgene #40730) (49)], and *3xflag* fused to the first 1,200 nucleotides of *sidI*
309 (3FLAG-SidI-F/3FLAG-SidI-R; from pSN85::*sidI*), which was ligated as a SacI/SalI fragment into
310 pSR47s to generate pSR47S::araBAD. Plasmids were transformed into chemically competent *E.*
311 *coli* DH5αλ*pir* and sequences were confirmed by Sanger sequencing (Eton Biosciences). To gen-
312 erate paraBAD strains, pSR47s::paraBAD was conjugated into *L. pneumophila* SRS43 wild type,
313 Δ*mesI*, and *sidI*$_{R453P}$Δ*mesI* (10) and selection of double crossover events was performed as described
314 (48). Sucrose resistant, kanamycin sensitive colonies were screened by PCR to verify gene inser-
315 tion.
316
317 **Mice.** C57Bl/6 *Nlrc4*$^{-/-}$ mice (a gift from Dr. Craig Roy) have been described (50). In-house colonies
318 were maintained under specific pathogen-free conditions at Kansas State University. Bone mar-
319 row was harvested from 8- to 15-week-old mice as previously described (51). All experiments
320 involving animals were approved by the Kansas State University Institutional Animal Care and
321 Use Committee (IACUC-4501 and -4022) and performed in compliance with the Animal Welfare
322 Act and National Institutes of Health guidelines.
323

324 **Cell culture.** All mammalian cells were grown at 37˚C/5% CO2. HEK293 FcγRII cells (a gift from
325 Dr. Craig Roy) were cultured in Dulbecco's Modified Eagle Medium (DMEM; Gibco) supple-
326 mented with 10% heat-inactivated fetal bovine serum (HIFBS; Biowest) for up to 25 passages.
327 Primary mouse bone marrow-derived macrophages (BMDMs) were differentiated in RPMI sup-
328 plemented with 20% HIFBS (Biowest) and 15% L-929 conditioned medium (Differentiation me-
329 dia) for 6 days prior to infection, as described (51). Differentiated BMDMs were seeded for infec-
330 tions in RMPI supplemented with 10%HIFBS and 7.5% L-929 conditioned medium (Seeding me-
331 dium).
332
333 **Macrophage growth curves.** BMDMs were seeded into 24-well tissue culture dishes at 2.5 x 10^5
334 per well one day prior to infection. *L. pneumophila* were cultured on CYE agar and heavy patch-
335 grown bacteria were used to infect BMDMs at a MOI of 1 in triplicates and CFU were enumerated
336 as previously described (10, 15). Fold growth was calculated by normalizing CFU at 24 h, 48 h,
337 and 72 h to internalized bacteria at 1 h post-infection. For genetic complementation, either 1 mM
338 IPTG or 2% L-arabinose (w/v) were added to the media as indicated at the time of infection and
339 maintained throughout.
340
341 ***In vitro* growth curves.** *L. pneumophila* heavy patches were resuspended in fresh AYE broth and
342 sub-cultured for consistent 600 nm optical density (OD_{600}). Cultures were split into triplicate wells
343 of a 96-well round-bottom plate and incubated at 37˚C with continuous orbital shaking using an
344 Agilent BioTek Epoch2 plate reader. OD_{600} from triplicate wells was read every two hours for 36

345 h. Plasmids were maintained with 10 μg mL^{-1} chloramphenicol and IPTG (1 mM) or 1% L-arabi-
346 nose (w/v) were added to the media to induce gene expression, as indicated.
347
348 **Quantitative RT-PCR.** *L. pneumophila* strains were grown for 1 or 6 h in AYE broth of incubation
349 with and without arabinose (2%), and total RNA was purified with the Direct-zol RNA miniprep
350 kit with TRI-reagent (Zymo Research) following manufacturer's instructions. RNA samples were
351 treated with DNase (Sigma) before reverse transcription with Superscript III (Invitrogen). Quan-
352 titative RT-PCR was performed using the Invitrogen SuperScript III Platinum SYBR Green One
353 Step qRT-PCR kit. Transcript abundance was quantified using sidIRT-F/sidIRT-R (sidI) and
354 16SRT-F/16SRT-R (16S rRNA) primer pairs on a BioRad CFX96 Real-Time PCR machine. Fold
355 expression (2^ΔΔCt) was calculated by normalizing *sidI* transcript abundance to 16S rRNA and
356 standardizing values to wild-type *L. pneumophila*.
357
358 **Bacterial viability and LIVE/DEAD staining.** *L. pneumophila* paraBAD strains were resuspended
359 in AYE media from a heavy patch (48 h). Strains were grown for 24 h at 37°C in the presence or
360 absence of 0.6% L-arabinose (w/v). Cell viability was quantified using a LIVE/DEAD™ *Bac-*
361 Light™ Bacterial Viability kit according to manufacturer's instructions. Bacteria were stained
362 with 5 μM SYTO9 (live; green) and 10 μM propidium iodide (dead; red) (ThermoFisher) and
363 incubated for 15 min at room temperature in the dark. To determine the baseline threshold for
364 dead cells a negative control was used, where cells were treated with 90% ethanol for 1 h. After
365 staining, cells were washed with sterile water and 5μL of resuspended cells were loaded on a
366 glass slide with a coverslip. Images were acquired at the KSU Division of Biology Microscopy

367 Facility using a Zeiss LSM5 Laser Scanning Confocal Microscope using a 100x oil-immersion ob-
368 jective. Percent dead bacteria was calculated by normalizing dead bacteria (red) to total bacteria
369 using ImageJ software. At least 500 cells were evaluated for each strain and culture condition and
370 the researcher performing the analysis was blinded to sample identity.
371
372 **Western blot.** Protein was boiled in Laemmli Buffer and separated by SDS-PAGE and were trans-
373 ferred to polyvinylidene difluoride (PVDF; Fisher Scientific) membranes using a BioRad wet
374 transfer apparatus. The membranes were incubated with blocking buffer [5% nonfat milk powder
375 dissolved in Tris-buffered saline-0.1% Tween 20 (TBST)] for 30 min. Membranes were incubated
376 with primary antibodies [mouse α-FLAG M2 (1:1000; Sigma); rabbit α-ICDH (1:1,000; Sigma);
377 rabbit α-β-actin (Cell Signaling); rabbit α-Myc TAG mAb (71D10) (1:1,000; Cell Signaling)] at
378 1:1,000 in blocking buffer overnight at 4˚C with rocking and subsequently with HRP-conjugated
379 goat α-rabbit or α-mouse secondary antibodies at 1:5,000 (ThermoFisher) in blocking buffer for 2
380 h at room temperature with rocking. Membranes were washed, incubated with ECL reagent (GE
381 Amersham), and imaged by chemiluminescence using an Azure Biosystems c300 Darkroom Re-
382 placer.
383
384 **Saponin solubilization assay.** HEK293 FcγRII cells (52) were seeded in 10 cm poly-L-lysine-
385 coated tissue culture dishes (4 x 10^6) one day prior to infection. *L. pneumophila* strains were
386 patched from fresh single colonies onto CYE agar supplemented with 10 μg mL^{-1} chlorampheni-
387 col and 1 mM IPTG to induce gene expression. Bacteria were opsonized with α-*L. pneumophila*
388 antibody [1:1,000 (Invitrogen; PA17227)] in DMEM 10%HIFBS supplemented with 1 mM IPTG

389 for 20 min at room temperature (RT) with rotation. Cells were infected with opsonized bacteria
390 at a MOI of 50 in for 2 h in 2 mL DMEM 10%HIFBS supplemented with 1 mM IPTG. Cells were
391 washed 3X with ice-cold PBS to remove extracellular bacteria and lysed for 10 min in 500 μL ice-
392 cold Hank's Balanced Salt Solution (HBSS) supplemented with 0.2% saponin and ProBlock™
393 Gold Mammalian Protease Inhibitor Cocktail (GoldBio). Lysates were treated with RNAse A (10
394 μg mL-1) and DNase I (10 μg mL-1), incubated at RT for 15 min, and centrifuged for 15 min at
395 17,000 r.c.f at 4˚C. Saponin-soluble supernatants were filtered using a 0.22 μM syringe filter and
396 transferred to a fresh 1.5 mL microcentrifuge tube. Saponin-insoluble pellets were resuspended
397 in 50 μL TE buffer (10 mM Tris-HCl, 1 mM EDTA). Fifty microliters of supernatant and pellet
398 fractions were diluted in 3X Laemmeli sample buffer, boiled for 10 min, and the whole sample
399 was loaded into wells of a 1.5 mm 15% SDS-PAGE gel for Western blot.
400
401 **Affinity chromatography.** Affinity chromatography from *E. coli* lysates was performed as de-
402 scribed (12). Briefly, *E. coli* BL21 (DE3) harboring pT7HMT::*mesI*, pT7HMT::*mesI*$_{\Delta 10}$,
403 pGEX6P1::sidI, or pGEX6P1 were grown overnight with shaking at 37˚C overnight and sub-cul-
404 tured at 1:100 in LB media. Sub-cultures were grown for 3 h followed by induction with 1 mM
405 IPTG and growth overnight at 16˚C. Clarified lysates from bacteria producing GST-fusion pro-
406 teins were incubated with pre-equilibrated glutathione magnetic agarose beads (Pierce) for 1h at
407 4˚C with rotation. Beads were washed twice in washing buffer (125 mM Tris-Cl, 150 mM NaCl,
408 1mM DTT, 1 mM EDTA, pH 7.4) and incubated with clarified lysates from bacteria producing
409 His$_6$-Myc fusion proteins at 4˚C for 1 h with rotation. Beads were washed twice in washing buffer
410 transferred to a fresh 1.5 mL microcentrifuge tube and boiled in 25 μM 3X Laemmli Sample buffer.

411 Proteins were separated by SDS-PAGE and visualized using Coomassie brilliant blue or Western
412 Blot, as indicated.
413
414 **Cytotoxicity Assay.** Cytotoxicity was evaluated by quantifying lactate dehydrogenase (LDH) ac-
415 tivity in supernatants of *L. pneumophila*-infected BMDMs. BMDMs were seeded in 24-well tissue
416 culture dishes at $2.5x10^5$ in Seeding medium one day prior to infection. Cells were infected with
417 *L. pneumophila* strains at an MOI of 50 for 1 h, washed 3 times with sterile phosphate-buffered
418 saline ($PBS^{-/-}$), and incubated in seeding media for additional 5 h or 9 h. At the indicated times,
419 plates were centrifuged at 250 r.c.f. and supernatants were transferred to a sterile non-tissue cul-
420 ture treated 96 well plate. For the 1 h timepoint, supernatants were collected from cells without
421 washing. LDH was quantified using the CytoTox™ 96 Non-radioactive Cytotoxicity Assay
422 (Promega) and according to manufacturer's instructions. Absorbance at 490 nm was read on a
423 BioTek Epoch2 microplate reader and percent cytotoxicity was calculated by normalizing absorb-
424 ance values to cells treated with lysis buffer.
425
426 **Quantification of bacterial degradation within macrophages.** BMDMs ($1 x 10^5$) were seeded on
427 poly-L-lysine-coated glass coverslips in 24-well tissue culture dishes one day prior to infection.
428 BMDMs were infected in triplicate wells with the indicated *L. pneumophila* strains at an MOI of 30
429 for 1 h or 8 h. For the 8 h timepoint, extracellular bacteria were removed after 1 h by washing
430 coverslips three times in $PBS^{-/-}$ and incubated with fresh media for 7 h. Coverslips were fixed in
431 3.7% paraformaldehyde for 15 min and permeabilized with ice-cold methanol. Coverslips were
432 stained with 1:1,000 rabbit α-*L. pneumophila* primary antibody (Invitrogen; PA17227) and 1:500

433 Alexa488-conjugated goat α-rabbit secondary antibody (ThermoFisher). Nuclei were stained with
434 1:2,000 Hoeshst (ThermoFisher) and coverslips were mounted on slides with ProLong™ Gold
435 Antifade Mountant (Invitrogen). Degraded and intact bacteria were scored blind on a Leica DMiL
436 LED inverted epifluorescence microscope (*n*=150 per strain and time point). Representative im-
437 ages were acquired at the KSU College of Veterinary Medicine Confocal Core using a Zeiss LSM
438 880 inverted confocal microscope and processed using Fiji ImageJ and Adobe Photoshop soft-
439 ware.
440
441 **Statistical analysis.** Statistical analysis was performed with GraphPad Prism 9 software using
442 unpaired two-tailed *t*-test with a 95% confidence interval. Unless otherwise indicated, data are
443 presented as mean ± standard deviation (s.d.) and statistical analysis was performed on tripli-
444 cate biological replicates.
445
446 **Acknowledgements**
447 We thank Dr. Craig Roy for providing *Nlrc4*$^{-/-}$ mice and Dr. Philip Hardwidge for critical review
448 of the manuscript and helpful discussions. This work was funded by NIH/NIGMS Center for
449 Biomedical Research Excellence Research Project Grants (P20GM130448 and P20113117; to S.R.S.),
450 an NIH/NIGMS Kansas-INBRE Postdoctoral Fellowship (P20GM103418; to D.C.), and start-up
451 funds from Kansas State University.
452
453
454

455 **References**

456 1. Horwitz MA, Silverstein SC. 1980. Legionnaires' disease bacterium (*Legionella pneumophila*)
457 multiples intracellularly in human monocytes. J Clin Investigation 66:441–50.

458 2. Park JM, Ghosh S, O'Connor TJ. 2020. Combinatorial selection in amoebal hosts drives the
459 evolution of the human pathogen *Legionella pneumophila*. Nat Microbiol 1–11.

460 3. Gomez-Valero L, Rusniok C, Carson D, Mondino S, Pérez-Cobas AE, Rolando M, Pasricha S,
461 Reuter S, Demirtas J, Crumbach J, Descorps-Declere S, Hartland EL, Jarraud S, Dougan G,
462 Schroeder GN, Frankel G, Buchrieser C. 2019. More than 18,000 effectors in the *Legionella* genus
463 genome provide multiple, independent combinations for replication in human cells. Proc Na-
464 tional Acad Sci 116:2265 2273.

465 4. Swanson MS, Isberg RR. 1995. Association of *Legionella pneumophila* with the macrophage en-
466 doplasmic reticulum. Infect Immun 63:3609–3620.

467 5. Horwitz MA. 1983. Formation of a novel phagosome by the Legionnaires' disease bacterium
468 (*Legionella pneumophila*) in human monocytes. The Journal of experimental medicine 158:1319
469 1331.

470 6. Chauhan D, Shames SR. 2021. Pathogenicity and Virulence of *Legionella*: Intracellular replica-
471 tion and host response. Virulence 12:1122–1144.

472 7. Berger KH, Isberg RR. 1993. Two distinct defects in intracellular growth complemented by a
473 single genetic locus in *Legionella pneumophila*. Mol Microbiol 7:7 19.

474 8. Joseph AM, Shames SR. 2021. Affecting the Effectors: Regulation of *Legionella pneumophila* Ef-
475 fector Function by Metaeffectors. Pathogens 10:108.

476 9. Kubori T, Shinzawa N, Kanuka H, Nagai H. 2010. *Legionella* metaeffector exploits host pro-
477 teasome to temporally regulate cognate effector. Plos Pathog 6:e1001216.

478 10. Shames SR, Liu L, Havey JC, Schofield WB, Goodman AL, Roy CR. 2017. Multiple *Legionella*
479 *pneumophila* effector virulence phenotypes revealed through high-throughput analysis of tar-
480 geted mutant libraries. Proc National Acad Sci 114(48):E10446-E10454

481 11. Shen X, Banga S, Liu Y, Xu L, Gao P, Shamovsky I, Nudler E, Luo Z. 2009. Targeting eEF1A
482 by a *Legionella pneumophila* effector leads to inhibition of protein synthesis and induction of host
483 stress response. Cell Microbiol 11:911 926.

484 12. Joseph AM, Pohl AE, Ball TJ, Abram TG, Johnson DK, Geisbrecht BV, Shames SR. 2020. The
485 *Legionella pneumophila* metaeffector Lpg2505 (MesI) regulates SidI-mediated translation inhibi-
486 tion and novel glycosyl hydrolase activity. Infect Immun 88(5):e00853-19.

487 13. Ren T, Zamboni DS, Roy CR, Dietrich WF, Vance RE. 2006. Flagellin-deficient *Legionella* mu-
488 tants evade caspase-1- and Naip5-mediated macrophage immunity. Plos Pathog 2:e18.

489 14. Molofsky AB, Byrne BG, Whitfield NN, Madigan CA, Fuse ET, Tateda K, Swanson MS. 2006.
490 Cytosolic recognition of flagellin by mouse macrophages restricts *Legionella pneumophila* infec-
491 tion. J Exp Med 203:1093 1104.

492 15. Ngwaga T, Hydock AJ, Ganesan S, Shames SR. 2019. Potentiation of Cytokine-Mediated Re-
493 striction of *Legionella* Intracellular Replication by a Dot/Icm-Translocated Effector. J Bacteriol
494 201:13.

495 16. Falkow S. 2004. Molecular Koch's postulates applied to bacterial pathogenicity — a personal
496 recollection 15 years later. Nat Rev Microbiol 2:67–72.

497 17. Falkow S. 1988. Molecular Koch's Postulates Applied to Microbial Pathogenicity. Clin Infect
498 Dis 10:S274–S276.

499 18. Faucher SP, Mueller CA, Shuman HA. 2011. *Legionella pneumophila* Transcriptome during In-
500 tracellular Multiplication in Human Macrophages. Front Microbiol 2:60.

501 19. McCloskey A, Perri K, Chen T, Han A, Luo Z-Q. 2021. The metaeffector MesI regulates the
502 activity of the *Legionella* effector SidI through direct protein-protein interactions. Microbes Infect
503 104794.

504 20. Burstein D, Zusman T, Degtyar E, Viner R, Segal G, Pupko T. 2009. Genome-Scale Identifica-
505 tion of *Legionella pneumophila* Effectors Using a Machine Learning Approach. Plos Pathog
506 5:e1000508.

507 21. Puvar K, Iyer S, Fu J, Kenny S, Terón KIN, Luo Z-Q, Brzovic PS, Klevit RE, Das C. 2020. *Le-*
508 *gionella* effector MavC targets the Ube2N~Ub conjugate for noncanonical ubiquitination. Nat
509 Commun 11:2365.

510 22. Liu Y, Luo Z-Q. 2007. The *Legionella pneumophila* effector SidJ is required for efficient recruit-
511 ment of endoplasmic reticulum proteins to the bacterial phagosome. Infect Immun 75:592 603.

512 23. Dalebroux ZD, Edwards RL, Swanson MS. 2009. SpoT governs *Legionella pneumophila* differ-
513 entiation in host macrophages. Mol Microbiol 71:640 658.

514 24. Creasey EA, Isberg RR. 2012. The protein SdhA maintains the integrity of the *Legionella*-con-
515 taining vacuole. Proc National Acad Sci 109:3481 3486.

516 25. Roy CR, Berger KH, Isberg RR. 1998. *Legionella pneumophila* DotA protein is required for
517 early phagosome trafficking decisions that occur within minutes of bacterial uptake. Mol Micro-
518 biol 28:663–674.

519 26. Benz J, Meinhart A. 2014. Antibacterial effector/immunity systems: it's just the tip of the ice-
520 berg. Curr Opin Microbiol 17:1–10.

521 27. Altindis E, Dong T, Catalano C, Mekalanos J. 2015. Secretome Analysis of *Vibrio cholerae*
522 Type VI Secretion System Reveals a New Effector-Immunity Pair. Mbio 6:e00075-15.

523 28. Kirchberger PC, Unterweger D, Provenzano D, Pukatzki S, Boucher Y. 2017. Sequential dis-
524 placement of Type VI Secretion System effector genes leads to evolution of diverse immunity
525 gene arrays in Vibrio cholerae. Sci Rep-uk 7:45133.

526 29. Yang X, Long M, Shen X. 2018. Effector–Immunity Pairs Provide the T6SS Nanomachine its
527 Offensive and Defensive Capabilities. Molecules 23:1009.

528 30. Feldman MF, Cornelis GR. 2003. The multitalented type III chaperones: all you can do with
529 15 kDa. Fems Microbiol Lett 219:151–158.

530 31. Belyi Y. 2020. Targeting Eukaryotic mRNA Translation by *Legionella pneumophila*. Frontiers
531 Mol Biosci 7:80.

532 32. Ganoza MC, Kiel MC, Aoki H. 2002. Evolutionary Conservation of Reactions in Translation.
533 Microbiol Mol Biol R 66:460–485.

534 33. Leon JAD, Qiu J, Nicolai CJ, Counihan JL, Barry KC, Xu L, Lawrence RE, Castellano BM,
535 Zoncu R, Nomura DK, Luo Z-Q, Vance RE. 2017. Positive and Negative Regulation of the Mas-
536 ter Metabolic Regulator mTORC1 by Two Families of *Legionella pneumophila* Effectors. Cell Re-
537 ports 21:2031–2038.

538 34. Belyi Y, Tartakovskaya D, Tais A, Fitzke E, Tzivelekidis T, Jank T, Rospert S, Aktories K.
539 2012. Elongation Factor 1A Is the Target of Growth Inhibition in Yeast Caused by *Legionella*
540 *pneumophila* Glucosyltransferase Lgt1. J Biol Chem 287:26029 26037.

541 35. Belyi Y, Tabakova I, Stahl M, Aktories K. 2008. Lgt: a family of cytotoxic glucosyltransferases
542 produced by *Legionella pneumophila*. J Bacteriol 190:3026 3035.

543 36. Qaidi SE, Scott NE, Hardwidge PR. 2021. Arginine glycosylation enhances methylglyoxal
544 detoxification. Sci Rep-uk 11:3834.

545 37. Qaidi SE, Scott NE, Hays MP, Geisbrecht BV, Watkins S, Hardwidge PR. 2020. An intra-bac-
546 terial activity for a T3SS effector. Sci Rep-uk 10:1073.

547 38. Qaidi SE, Scott NE, Hays MP, Hardwidge PR. 2022. Arginine glycosylation regulates UDP-
548 GlcNAc biosynthesis in Salmonella enterica. Sci Rep-uk 12:5293.

549 39. Hasan MK, Qaidi SE, Hardwidge PR. 2021. The T3SS Effector Protease NleC Is Active within
550 *Citrobacter rodentium*. Pathogens 10:589.

551 40. Bertram R, Schuster CF. 2014. Post-transcriptional regulation of gene expression in bacterial
552 pathogens by toxin-antitoxin systems. Front Cell Infect Mi 4:6.

553 41. Machtens DA, Willerding JM, Eschenburg S, Reubold TF. 2020. Crystal structure of the
554 metaeffector MesI (Lpg2505) from *Legionella pneumophila*. Biochem Bioph Res Co 527:696–701.

555 42. Hugoson E, Guliaev A, Ammunét T, Guy L. 2022. Host-adaptation in *Legionellales* is 1.9 Ga,
556 coincident with eukaryogenesis. Mol Biol Evol 2;39(3)msac037

557 43. Feeley JC, Gibson RJ, Gorman GW, Langford NC, Rasheed JK, Mackel DC, Baine WB. 1979.
558 Charcoal-yeast extract agar: primary isolation medium for *Legionella pneumophila*. J Clin Micro-
559 biol 10:437 441.

560 44. Saito A, Rolfe RD, Edelstein PH, Finegold SM. 1981. Comparison of liquid growth media for
561 *Legionella pneumophila*. J Clin Microbiol 14:623 627.

562 45. Merriam JJ, Mathur R, Maxfield-Boumil R, Isberg RR. 1997. Analysis of the *Legionella pneu-*
563 *mophila fliI* gene: intracellular growth of a defined mutant defective for flagellum biosynthesis.
564 Infect Immun 65:2497–2501.

565 46. Folly-Klan M, Alix E, Stalder D, Ray P, Duarte LV, Delprato A, Zeghouf M, Antonny B,
566 Campanacci V, Roy CR, Cherfils J. 2013. A novel membrane sensor controls the localization and
567 ArfGEF activity of bacterial RalF. Plos Pathog 9:e1003747.

568 47. Geisbrecht BV, Bouyain S, Pop M. 2006. An optimized system for expression and purifica-
569 tion of secreted bacterial proteins. Protein Expres Purif 46:23–32.

570 48. Bardill JP, Miller JL, Vogel JP. 2005. IcmS-dependent translocation of SdeA into macrophages
571 by the *Legionella pneumophila* type IV secretion system. Mol Microbiol 56:90 103.

572 49. Blakeley BD, Chapman AM, McNaughton BR. 2012. Split-superpositive GFP reassembly is a
573 fast, efficient, and robust method for detecting protein-protein interactions *in vivo*. Mol Biosyst
574 8:2036 2040.

575 50. Lara-Tejero M, Sutterwala FS, Ogura Y, Grant EP, Bertin J, Coyle AJ, Flavell RA, Galán JE.
576 2006. Role of the caspase-1 inflammasome in *Salmonella typhimurium* pathogenesis. J Exp Med
577 203:1407 1412.

578 51. Case CL, Roy CR. 2013. Analyzing caspase-1 activation during *Legionella pneumophila* infec-
579 tion in macrophages. Methods Mol Biol (Clifton, NJ) 954:479 491.

580 52. Arasaki K, Roy CR. 2010. *Legionella pneumophila* promotes functional interactions between
581 plasma membrane syntaxins and Sec22b. Traffic Cph Den 11:587–600.

582

583 **Tables**

584 **Table 1.** Plasmids used in this study

Name	Description	Resistance	Ref/Source
Protein production			
pT7HMT	Production of His_6-Myc fusions	Kan^R	(47)
pT7HMT::*mesI*	Production of His_6-Myc-MesI	Kan^R	(12)
pT7HMT::$mesI_{\Delta 10}$	Production of His_6-Myc-MesIΔ10	Kan^R	This study
pGEX6P1	Production of GST	Amp^R	GE healthcare
pGEX6P1::*sidI*	Production of GST-SidI	Amp^R	(12)
Allelic exchange			
pSR47s	Allelic exchange vector	Kan^R	(48)
pSR47s::*paraBAD*	For chromosomal integration of *araBAD-3xflag* upstream of *sidI*	Kan^R	This study
pSR47s::Δ*dotA*	For in-frame deletion of *dotA*	Kan^R	This study
Genetic complementation and cloning			
pJB1806	*Legionella* expression vector		(45)
pJB1806::*sidI* (p*sidI*)	*sidI* expression from P*tac*	Cm^R	This study
pJB1806::$sidI_{R453P}$ (p$sidI_{RP}$)	$sidI_{R453P}$ expression from P*tac*	Cm^R	This study
pSN85	*Legionella* vector with in-frame N-terminal *3xflag* epitope tag		(46)
pSN85::*sidI*	To generate *3xflag-sidI*	Cm^R	This study
pSN85::*mesI* (p*mesI*)	*3xflag-mesI* expression from P*tac*	Cm^R	This study
pSN85::$mesI_{\Delta 10}$ (p$mesI_{\Delta 10}$)	*3xflag-*$mesI_{\Delta 10}$ expression from P*tac*	Cm^R	This study

585

586 **Table 2**. Oligonucleotide primers used in this study

Name	Sequence[a]
Protein production	
MesIT7SalI-F	att**gtcgac**aatgataaaaggaaaacttatgccc
MesIΔ10NotI-R	att**gcggccgc**ttactcatcgtctttacc
Allelic exchange	
DotAKOSacI-F	attgtcgacgccctagctgtttcattgc
DotAKONotI-R	attgcggccgcacattctttctcacccaataac
DotAKONotI-F	att**gcggccgca**taacattcaaaaacaatata
DotAKOSalI-R	att**gagctc**ccaaaacaaaataaccagctg
SidIUTR-F	ccccc**gagctc**gagcatcaataatatcctgc
SidIUTR-R	gtagccgtcaagttgtcaaaattactttagtaaaatttttgtcatggtg

araC-pBAD-F	caccatgacaaaaattttactaaagtaattt tgacaacttgacggctacatc
araC-pBAD-R	catggtctttgtagtccat)atatctccttcttaaagttaaacaaaattatttc
3FlagSidI-F	gtttaactttaagaaggagatatatggactacaaagaccatgacg
3FlagSidI-R	ccccc**gtcgac**tgactacacccctctttattggc
Genetic complementation	
SidIBamHI-F	tta**ggatcc**ttatgactaaaatatacttattaac
SidISphI-R	att**gcatgc**tcaatcacaaattaatttttgcacatc
MesIBglII-F	tgg**agatct**ttatgataaaaggaaaacttatgc
MesISphI-R	att**gcatgc**ttataaaataattggtcgag
MesIΔ10SphI-R	att**gcatgc**ttactcatcgtctttaccagc
qRT-PCR	
sidIRT-F	atcaggcaaaccgacgtgac
sidIRT-R	ccgcaatctggtggacgaat
16SRT-F	tcagtggggaggagggttga
16SRT-R	cgctcgcaccctccgtatta
Site-directed mutagenesis	
SidIR453P-sense	ccgcaatctggtggaggaatatgaatatcaagatgagta
SidIR453P-asense	tactcatcttgatattcatattcctccaccagattgcgg

587 a-Restriction endonuclease cleavage sites are **bolded**.
588

589 **Figures**

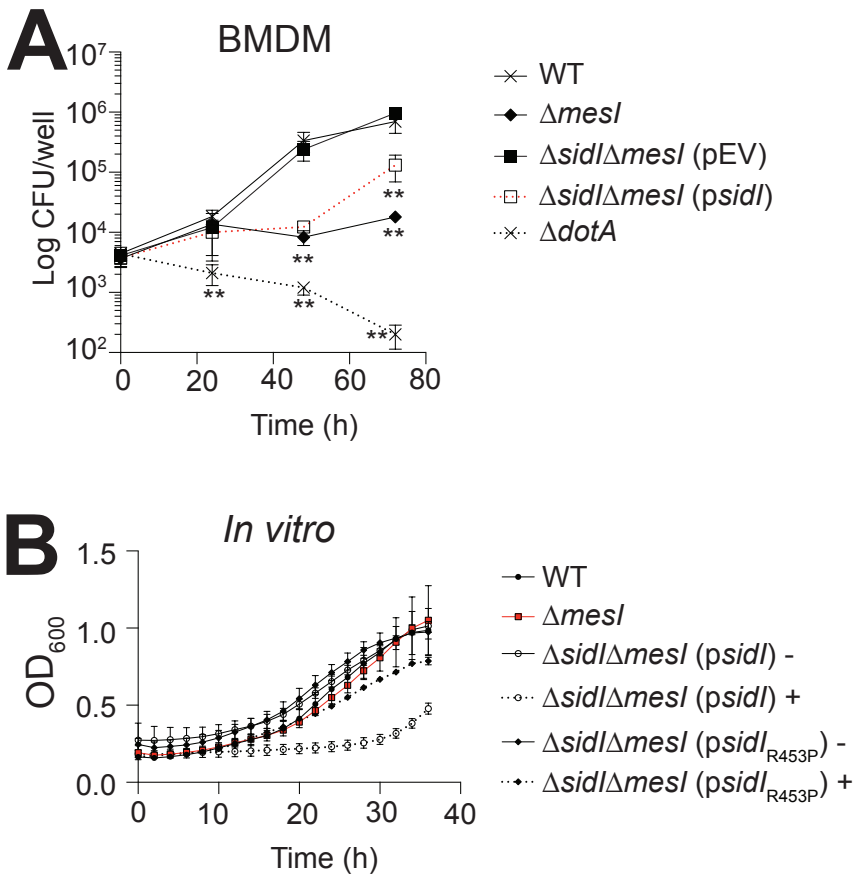

590

591

592 **Figure 1. Overexpression of *sidI* attenuates *L. pneumophila* replication. (A)** Fold replication of

593 *L. pneumophila* strains within *Nlrc4*$^{-/-}$ BMDMs over 72 h. Where indicated, infections were per-

594 formed in the presence of 1 mM IPTG. Data shown are mean ± s.d. on samples in triplicates and

595 asterisks denote statistical significance by Students' *t*-test (**P<0.01). **(B)** Optical density at 600 nm

596 (OD_{600}) of *L. pneumophila* strains grown in AYE broth. Where indicated, bacteria were grown in

597 the presence (+) or absence (-) of 1 mM IPTG. Data shown are mean ± s.d. on samples in triplicates

598 and asterisks denote statistical significance by Students' *t*-test (**P<0.01). Data shown are repre-

599 sentative of at least three independent experiments.

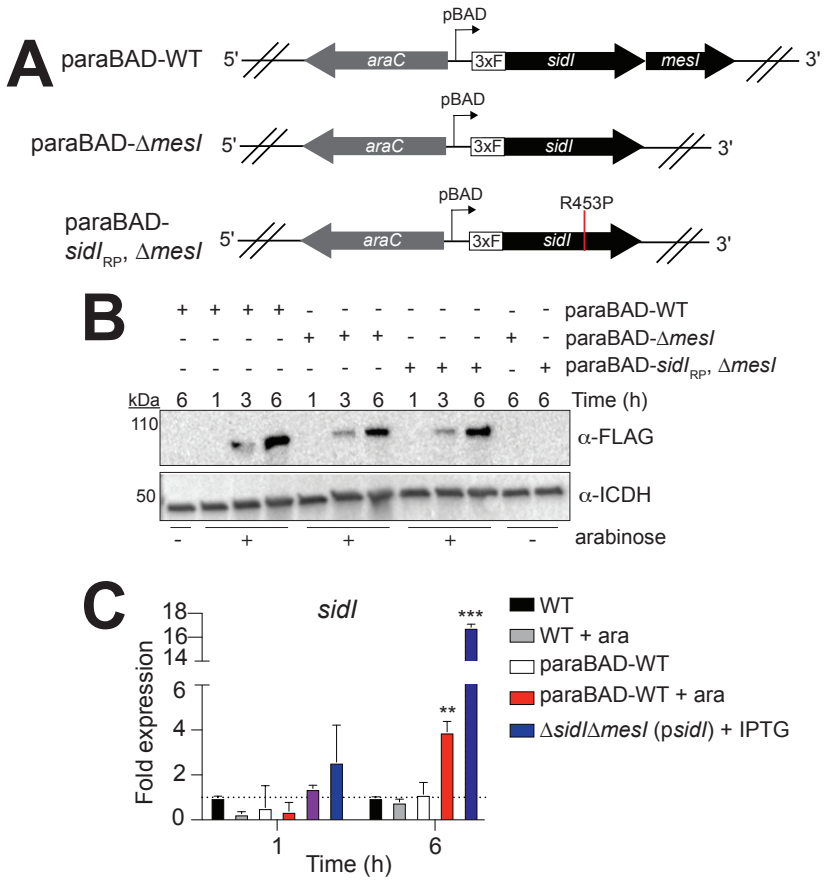

Figure 2. Establishment of a chromosomal arabinose-inducible expression system in *L. pneumophila*. (A) Schematic showing paraBAD insertion upstream of the sidI locus in the *L. pneumophila* chromosome. 3XF: In-frame *3xflag* epitope tag. **(B)** Western blot showing 3xFLAG-SidI production in the indicated paraBAD strains in the presence (+) or absence (-) of arabinose [ara; 0.6% (w/v)] after growth in AYE broth for 1, 3, or 6 h. **(C)** Quantitative RT-PCR for expression of *sidI* grown for 1 or 6 h in AYE broth. Fold expression in OD-normalized cultures (n = 3) was calculated relative to wild-type *L. pneumophila* at each time point. Asterisks denote statistical significance by Students' t-test (**P<0.01) on samples in triplicates. Data are representative of at least two independent experiments.

611

612

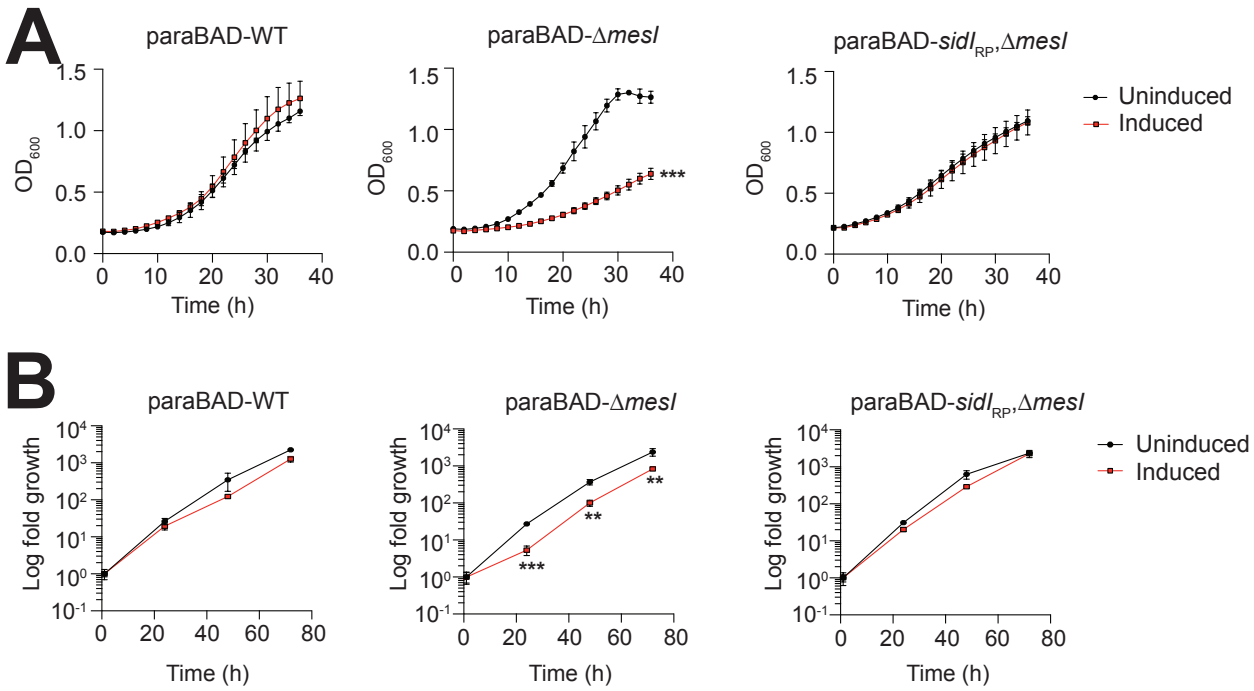

613

614

615 **Figure 3. SidI impairs *L. pneumophila* growth when uncoupled from MesI. (A)** Replication of

616 the *L. pneumophila* paraBAD strains grown in AYE broth *in vitro* under inducing [1% arabinose

617 (w/v)] or noninducing conditions. Data shown are mean ± s.d. OD600 values from samples in

618 triplicates and asterisks denote statistical significance by Students' t-test (**P<0.01). **(B)** Fold rep-

619 lication of *L. pneumophila* strains within *Nlrc4*$^{-/-}$ BMDMs under inducing [2% arabinose (w/v)] or

620 noninducing conditions. Data shown are mean ± s.d. on samples in triplicates and asterisks de-

621 note statistical significance by Students' *t*-test (**P<0.01). Data shown are representative of at least

622 three independent experiments.

623

624

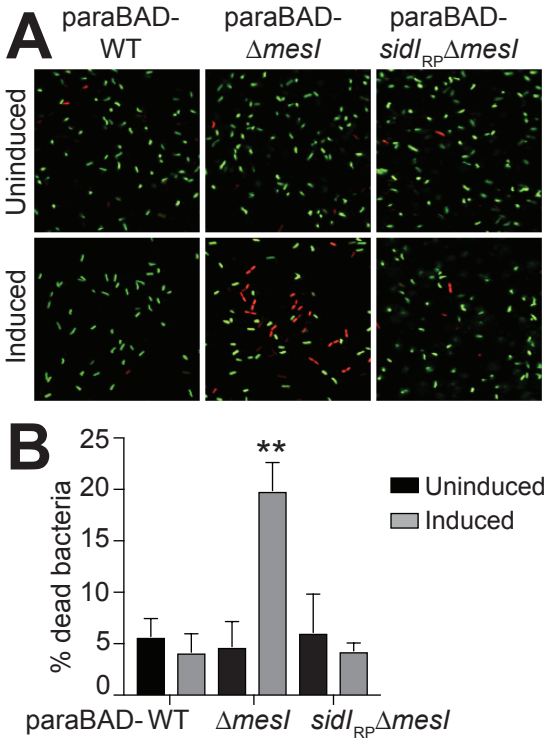

Figure 4. SidI is bactericidal in the absence of MesI. (A) Representative confocal micrographs of Live/Dead-stained *L. pneumophila* paraBAD strains grown in AYE broth under inducing [0.6% arabinose (w/v)] or noninducing conditions [SYTO9 (live; green) and propidium iodide (PI; dead; red)]. **(B)** Quantification of dead *L. pneumophila* by fluorescence microscopy following Live/Dead staining. Percent dead bacteria was calculated by dividing PI-stained cells by total cells. Data are mean ± s.d. of 650 cells scored blind and asterisks denote statistical significance by Students' *t*-test (**P<0.01). Data are representative of two independent experiments.

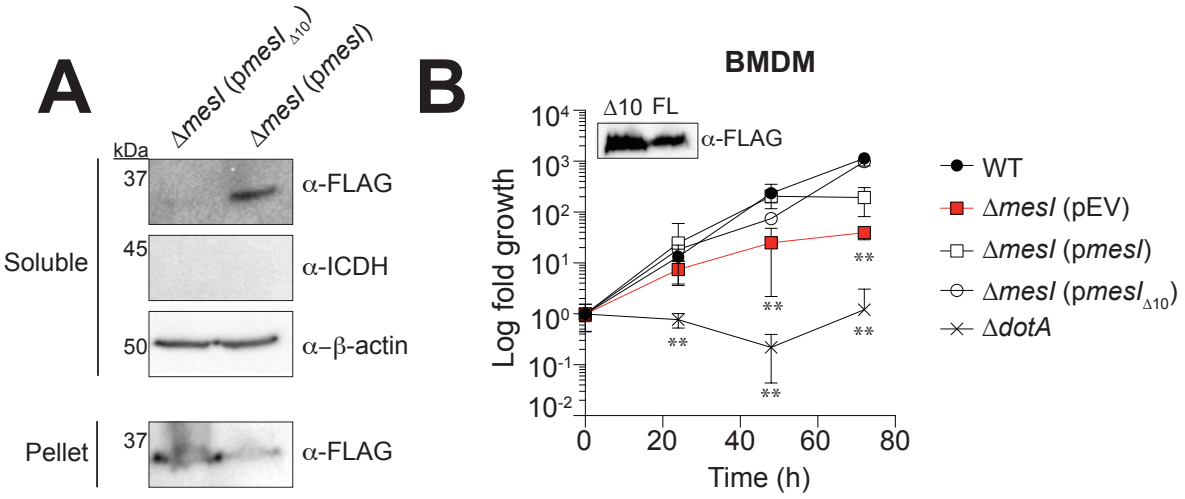

638

639

640 **Figure 5. MesI translocation is dispensable for *L. pneumophila* intracellular replication. (A)**
641 Western blot for 3xFLAG-MesI fusion proteins in saponin-solubilized lysates of HEK293 FcγRII
642 cells infected with antibody-opsonized *L. pneumophila* Δ*mesI* harboring p*mesI* (3xFLAG-MesI) or
643 p*mesI*$_{\Delta 10}$ (3xFLAG-MesIΔ10). Expression of 3xFLAG-MesI fusions was confirmed by Western blot
644 on saponin-insoluble pellets. ICDH and β-actin were used as controls for bacterial lysis and equal
645 loading, respectively. Data are representative of three independent experiments. **(B)** Replication
646 of *L. pneumophila* strains within *Nlrc4*$^{-/-}$ BMDMs infected at an MOI of 1. Fold growth was calcu-
647 lated by normalizing CFU counts to internalized bacteria at 1 h post-infection. Plasmid expression
648 of *mesI* alleles was induced with 1 mM IPTG and confirmed by Western blot (inset). Asterisks
649 denote statistical significance (**P<0.05) by Students' t-test on samples in triplicates. Data are rep-
650 resentative of three independent experiments.

651

652

653

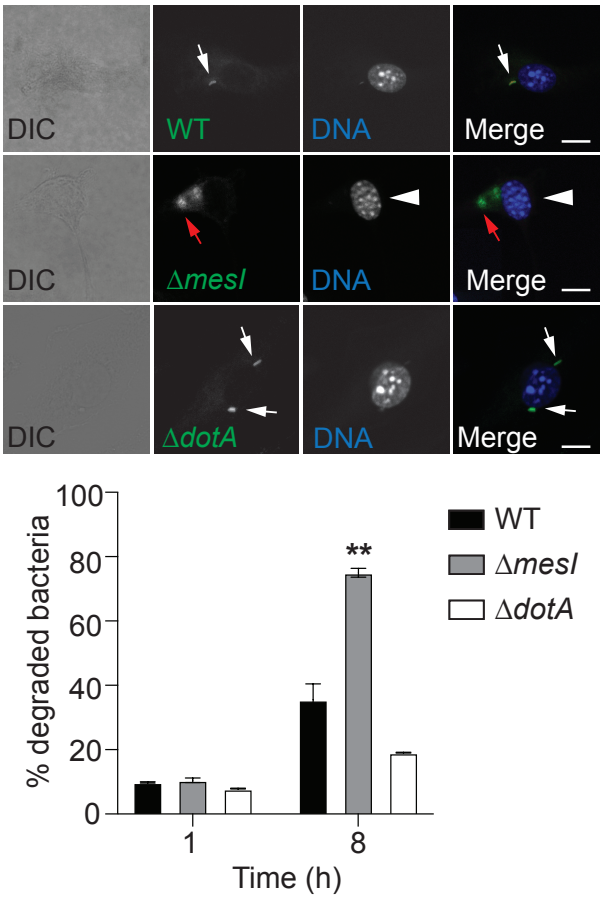

654

655 **Figure 6. MesI-deficient bacteria are efficiently degraded in host cells. (Top)** Representative

656 confocal micrographs of *Nlrc4*$^{-/-}$ BMDMs infected for 8 h (MOI of 30) with *L. pneumophila* wild-

657 type (WT), Δ*mesI*, or Δ*dotA*. Intact and degraded bacteria (green) are indicated with white and

658 red arrows, respectively. Nuclei of Δ*mesI*-infected BMDMs are indicated with white arrowhead.

659 Scale bar is 10 μm. **(Bottom)** Quantification of degraded *L. pneumophila* within *Nlrc4*$^{-/-}$ BMDMs

660 infected for 1 or 8 h at an MOI of 30. were infected with *L. pneumophila.* Percent degraded bacte-

661 ria were enumerated by blinded immunofluorescence scoring of samples in triplicates (n = 300).

662 Asterisks denote statistical significance (**P<0.01) by Students' t-test and data shown are repre-

663 sentative of two independent experiments.

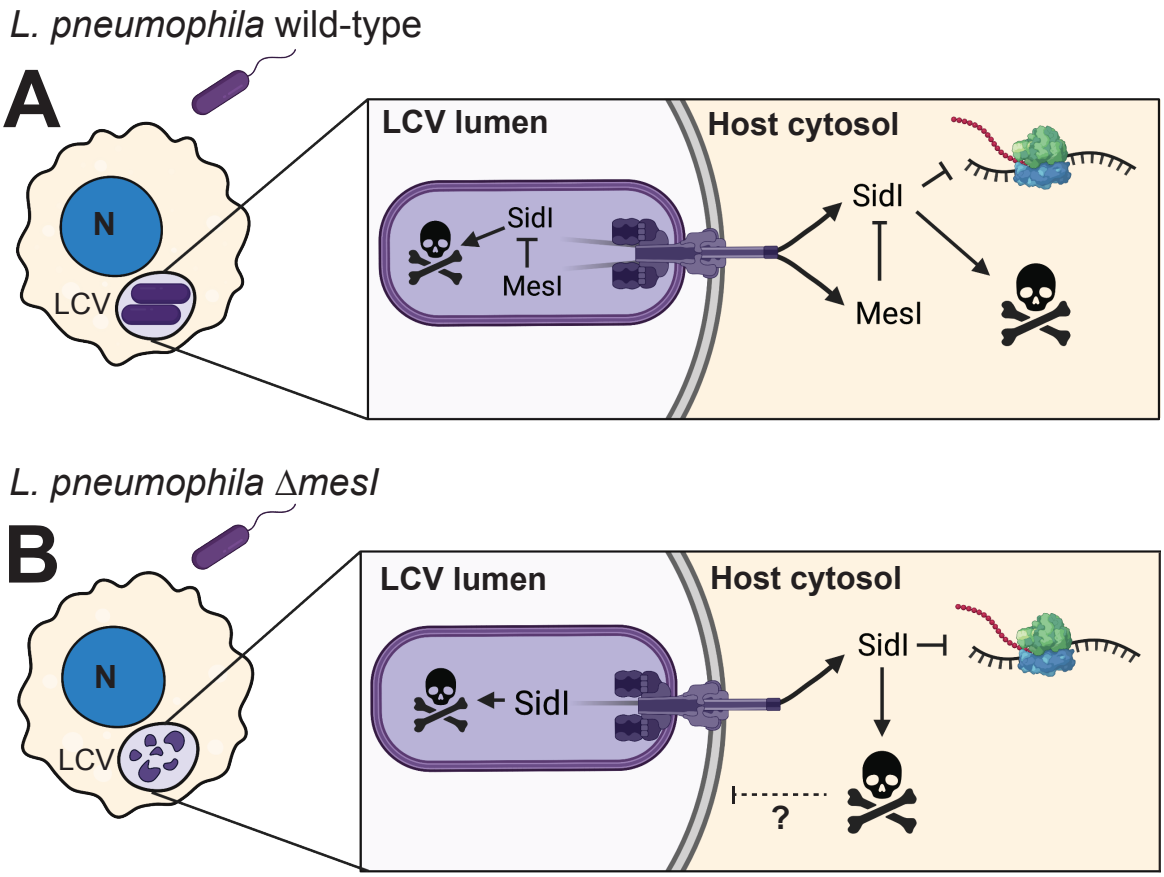

Figure 7. Model for the MesI regulatory mechanism. (A) MesI regulates SidI toxicity within host cells and the bacterium promotes replication of virulent *L. pneumophila* (purple) within host cells by regulating SidI within the bacterium and host cell. SidI inhibits eukaryotic protein synthesis and is toxic to both host cells and *L. pneumophila* in the absence of MesI. **(B)** MesI-deficient bacteria are degraded within host cells, which is likely a consequence of intrabacterial SidI toxicity. A role for SidI host cell toxicity in the *L. pneumophila ΔmesI* virulence defect is unclear (dashed line). Figure created with Biorender.com.

675 **Supplemental Figures**

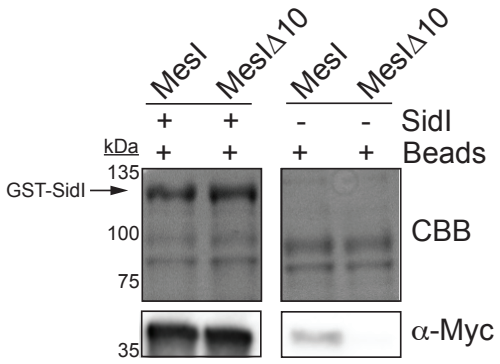

676

677 **Figure S1. MesIΔ10 binds SidI.** Glutathione agarose beads were incubated with lysates from *E.*

678 *coli* producing GST-SidI or GST (beads) and subsequently incubated with lysates from *E. coli* pro-

679 ducing His_6-Myc-MesI or -MesIΔ10. Proteins on beads were separated by SDS-PAGE and visual-

680 ized by Coomassie brilliant blue (CBB) staining or α-Myc Western blot, as indicated. Data are

681 representative of three independent experiments.

682

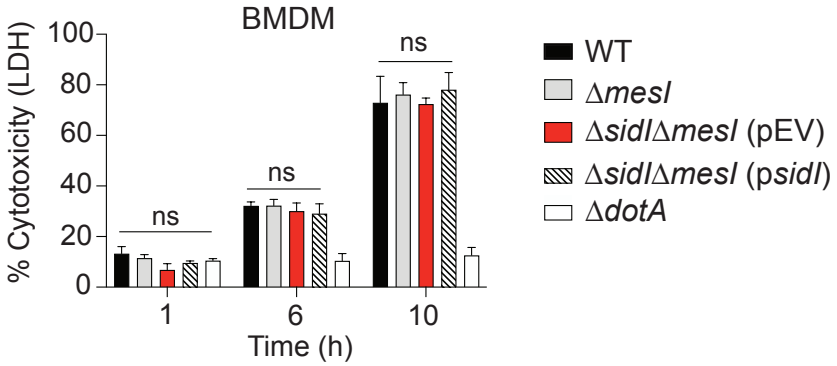

683

684 **Figure S2. Host cell death is not increased by SidI-producing *L. pneumophila*.** Lactate dehy-

685 drogenase activity in supernatants of *Nlrc4*$^{-/-}$ BMDMs infected with the indicated *L. pneumophila*

686 strains (MOI of 30) for 1, 6, or 10 h. Plasmid expression of *sidI* was induced with 1 mM IPTG.

687 Data are representative of three independent experiments and statistical analysis was per-

688 formed using Students' *t*-test (ns, not significant).